SIAM J. APPL. MATH.
Vol. 69, No. 6, pp. 1542–1558

INTERACTIONS OF ELEMENTARY WAVES FOR THE AW–RASCLE MODEL*

MEINA SUN†

Abstract. In this paper, we study the interactions of elementary waves for the traffic flow model proposed by Aw and Rascle in [*SIAM J. Appl. Math.*, 60 (2000), pp. 916–938]. The solutions are obtained constructively when the initial data are three piecewise constant states. In particular, a new wave SJ in which a shock wave S and a contact discontinuity J coincide with each other is obtained during the process of interaction. Moreover, by studying the limits of the solutions as the perturbed parameter ε tends to zero, it can be found that the Riemann solutions are stable for such perturbations with the initial data.

Key words. interaction of elementary waves, vacuum state, Aw–Rascle model, Riemann problem, traffic flow, hyperbolic conservation laws

AMS subject classifications. 35L65, 35L67, 35B30

DOI. 10.1137/080731402

1. Introduction.

The Aw–Rascle (AR) macroscopic model of traffic flow in the conservative form [2] is given by

$$\begin{cases} \rho_t + (\rho u)_x = 0, \\ (\rho(u + p(\rho)))_t + (\rho u(u + p(\rho)))_x = 0, \end{cases} \tag{1.1}$$

where ρ, u represent the density and the velocity, respectively; the velocity offset p takes the form $p(\rho) = \rho^\gamma$ with $\gamma > 0$. The AR model describes a traffic flow model on a unidirectional roadway. The basic assumptions of the model are the density $\rho(x,t) \geq 0$ and velocity $u(x,t) \geq 0$ of cars located at position x at time t.

The AR model was proposed in order to remedy the deficiencies of second order models of car traffic pointed out by Daganzo [6] and has been independently derived by Zhang [20]. The derivation of the model from a microscopic follow-the-leader (FL) model through a scaling limit was also given in [1]. The AR model resolves all the obvious inconsistencies and explains instabilities in the car traffic flow, especially near the vacuum, i.e., for very light traffic with few slow drivers [2, 11].

The AR model is one of the main fluid dynamic models for traffic flow and is appropriate for describing traffic phenomena, such as congestion and stop-and-go waves [10]. It is now widely used to study the formation and dynamics of traffic jams and is endowed with desirable stability properties. It is also the basis for the multilane traffic flow model [8, 9], the model for a road network with unidirectional flow [7, 10], and the hybrid traffic flow model [13].

In [3], the limit behavior was investigated by changing p into εp and taking $p(\rho) = (\frac{1}{\rho} - \frac{1}{\rho^*})^{-\gamma}$ with the density constraint $\rho \leq \rho^*$, where the maximal density ρ^* corresponds to a total traffic jam and is assumed to a fixed constant although

*Received by the editors July 28, 2008; accepted for publication (in revised form) November 17, 2008; published electronically March 4, 2009. This work was supported by National Natural Science Foundation of China.

http://www.siam.org/journals/siap/69-6/73140.html

†School of Mathematics and Information, Ludong University, Yantai, Shandong 264025, People's Republic of China, and Laboratory of Mathematics Physics, Wuhan Institute of Physics and Mathematics, The Chinese Academy of Sciences, Wuhan 430071, People's Republic of China (smnwhy0350@163.com).

it should depend on the velocity in practice. They discovered that the pressure term becomes active so as to preserve the constraint $\rho \le \rho^*$ when ρ reaches ρ^*. Recently, Shen and Sun [15] have considered the limit behavior without the constraint of the maximal density, i.e., $p(\rho)$ is not singular at $\rho = \rho^*$. The delta-shock wave was obtained through perturbing the pressure $p(\rho)$ suitably.

For convenience and conciseness, we replace $\rho p(\rho)$ with $p(\rho)$ in (1.1) and take $p(\rho) = \rho^\gamma$ for $\gamma > 1$; then the AR model can be rewritten in the following form:

$$\begin{cases} \rho_t + (\rho u)_x = 0, \\ (\rho u + \rho^\gamma)_t + (\rho u^2 + \rho^\gamma u)_x = 0. \end{cases} \tag{1.2}$$

In the above equations, $p(\rho) = \rho^\gamma$ can be regarded as the traffic pressure term and γ is analogous with the adiabatic gas constant in gas dynamics.

In this paper, our main purpose is to investigate various possible interactions of elementary waves for the AR model (1.2). To include all kinds of interactions, it suffices to consider the AR model (1.2) with the following perturbed initial data:

$$(u,\rho)(x,0) = \begin{cases} (u_-,\rho_-), & -\infty < x < -\varepsilon, \\ (u_m,\rho_m), & -\varepsilon < x < \varepsilon, \\ (u_+,\rho_+), & \varepsilon < x < +\infty, \end{cases} \tag{1.3}$$

where $\varepsilon > 0$ is arbitrarily small. We notice that (1.3) is a local perturbation of the Riemann data and we still call it a small perturbation here for ε is sufficiently small.

Aw and Rascle have investigated the Riemann problem of (1.1) in detail. With these results in mind, one would naturally like to study the interactions of elementary waves because they embody the internal mechanism of the AR model. Another motivation of this study comes from the fact that small changes in traffic flow will propagate and lead to the occurrence of wave interaction. Finally, the stability of the Riemann solutions of (1.2) can be analyzed if we take the initial data (1.3) and then let $\varepsilon \to 0$.

By definition, a vacuum state is any portion of the (x,t) plane in which $\rho = 0$. From [2], we know that the Riemann solutions do involve the vacuum state for certain Riemann data. In order to cover all the cases completely, we divide our work into two parts according to the presence of vacuum or not. When the vacuum is not involved, the problem about the interactions of elementary waves is classical and will not be addressed here. On the other hand, the AR model suitably explains instabilities near the vacuum. Therefore, we especially pay attention to the vacuum problem and consider the interactions of elementary waves in full detail when the vacuum is involved. Dealing with the vacuum problem, we adopt the idea proposed by Liu and Smoller [12] when they considered it for the isentropic gas dynamic equations, where they made a distinction between two vacuum states with different (fake) velocities.

With the method of characteristic analysis, the interactions are widely investigated and the global solutions are completely constructed. Furthermore, we find that the solutions of the perturbed initial value problem (1.2) and (1.3) converge to the solutions of the corresponding Riemann problem (1.2) and (2.1) as $\varepsilon \to 0$, which shows the stability of the Riemann solutions for certain perturbations of the initial data. Especially, when the vacuum is involved, the interesting feature in the solutions is that a new wave SJ is discovered during the interaction of a contact discontinuity J and a shock S in a particular situation. Here SJ is the superposition of a contact discontinuity and a shock. The reason for the generation of the wave SJ is due to the

fact that the newly formed waves S and J after interaction propagate with the same speed and coincide with each other.

For basic references on nonlinear hyperbolic systems of conservation laws and the interactions of elementary waves, we refer the readers to the book of Smoller [17] and the monograph of Chang and Hsiao [4]. Furthermore, one can see the books written by Dafermos [5] and Serre [14] for a comprehensive survey. Also see [16, 18] for the recent work about the interactions of elementary waves.

This paper is organized as follows. In section 2, we restate the Riemann problem to the AR model (1.2) for readers' convenience. In section 3, we mainly discuss the interactions of elementary waves when the vacuum is involved. In section 4, we consider the stability of the Riemann solutions under the small perturbations and compare our results with those of Aw and Rascle before our conclusion in section 5.

2. Preliminaries. In this section, we briefly review the Riemann solutions of (1.2) with the initial data

$$(u,\rho)(x,0) = (u_\pm,\rho_\pm), \qquad \pm x > 0, \tag{2.1}$$

where $u_\pm, \rho_\pm > 0$, and the detailed study can be found in [2].

The characteristic roots of system (1.2) are

$$\lambda_1 = u - (\gamma-1)\rho^{\gamma-1}, \qquad \lambda_2 = u; \tag{2.2}$$

therefore (1.2) is strictly hyperbolic except for $\rho = 0$.

The corresponding right characteristic vector of $\lambda_i (i = 1, 2)$ is

$$\overrightarrow{r_1} = ((1-\gamma)\rho^{\gamma-2}, 1)^T, \qquad \overrightarrow{r_2} = (0,1)^T. \tag{2.3}$$

It is easy to see that $\nabla\lambda_1 \cdot \overrightarrow{r_1} \neq 0$ for $\rho \neq 0$ and $\nabla\lambda_2 \cdot \overrightarrow{r_2} \equiv 0$ in which ∇ denotes the gradient with respect to (u,ρ); namely, λ_1 is genuinely nonlinear for $\rho \neq 0$ and λ_2 is always linearly degenerate. Therefore, the associated waves are rarefaction waves or shocks for the first family and contact discontinuities for the second family.

The Riemann invariants along the characteristic fields are

$$w = u + \rho^{\gamma-1}, \qquad z = u. \tag{2.4}$$

Since (1.2) and the Riemann data (2.1) are invariant under stretching of coordinates: $(x,t) \to (\alpha x, \alpha t)$ (α is constant), we seek the self-similar solution

$$(u,\rho)(x,t) = (u,\rho)(\xi), \qquad \xi = x/t. \tag{2.5}$$

Then the Riemann problem is reduced to the boundary value problem of the ordinary differential equations:

$$\begin{cases} -\xi\rho_\xi + (\rho u)_\xi = 0, \\ -\xi(\rho u + \rho^\gamma)_\xi + (\rho u^2 + \rho^\gamma u)_\xi = 0, \end{cases} \tag{2.6}$$

with $(u,\rho)(\pm\infty) = (u_\pm, \rho_\pm)$.

For smooth solutions, setting $U = (u,\rho)^T$, (2.6) can then be rewritten as

$$A(U)U_\xi = 0, \tag{2.7}$$

where

$$A(u,\rho)=\begin{pmatrix} \rho & u-\xi \\ -\xi\rho+2\rho u+\rho^{\gamma} & -\xi u-\gamma\xi\rho^{\gamma-1}+u^2+\gamma\rho^{\gamma-1}u \end{pmatrix}.$$

Besides the constant state solution, it provides a rarefaction wave which is a continuous solution of (2.7) in the form $(u,\rho)(\xi)$. Then, for a given left state (u_-,ρ_-), the rarefaction wave curves in the phase plane, which are the sets of states that can be connected on the right by a 1-rarefaction wave, are as follows:

$$R(u_-,\rho_-):\begin{cases} \xi=\lambda_1=u-(\gamma-1)\rho^{\gamma-1}, \\ u-u_-=-\rho^{\gamma-1}+\rho_-^{\gamma-1}, \\ \rho<\rho_-, \qquad u>u_-. \end{cases} \tag{2.8}$$

Through differentiating u with respect to ρ in the second equation in (2.8), we get

$$u_\rho=-(\gamma-1)\rho^{\gamma-2}, \qquad u_{\rho\rho}=-(\gamma-1)(\gamma-2)\rho^{\gamma-3}. \tag{2.9}$$

Thus the 1-rarefaction wave curve is convex for $1<\gamma<2$ and concave for $\gamma>2$ in the (u,ρ) plane.

For a bounded discontinuity at $\xi=\sigma$, the Rankine–Hugoniot condition holds:

$$\begin{cases} -\sigma[\rho]+[\rho u]=0, \\ -\sigma[\rho u+\rho^{\gamma}]+[\rho u^2+\rho^{\gamma}u]=0, \end{cases} \tag{2.10}$$

where $[\rho]=\rho_r-\rho_l$, $\rho_l=\rho(\sigma-0)$, and $\rho_r=\rho(\sigma+0)$, etc.

From the first equation in (2.10), we obtain

$$\rho_r(u_r-\sigma)=\rho_l(u_l-\sigma). \tag{2.11}$$

Simplifying the second equation in (2.10) and noting (2.11), it yields

$$\rho_r(u_r-\sigma)(u_r+\rho_r^{\gamma-1}-u_l-\rho_l^{\gamma-1})=0. \tag{2.12}$$

If $\rho_r(u_r-\sigma)\neq 0$, we have $u_r+\rho_r^{\gamma-1}=u_l+\rho_l^{\gamma-1}$, and the Lax entropy conditions imply that $\rho_l<\rho_r$. So for a given left state (u_-,ρ_-), the sets of states which can be connected to (u_-,ρ_-) by a 1-shock wave on the right are as follows:

$$S(u_-,\rho_-):\begin{cases} \sigma=u-\dfrac{\rho_-(\rho^{\gamma-1}-\rho_-^{\gamma-1})}{\rho-\rho_-}, \\ u-u_-=-\rho^{\gamma-1}+\rho_-^{\gamma-1}, \\ \rho>\rho_-, \qquad u<u_-. \end{cases} \tag{2.13}$$

It is noted that the shock curves coincide with the rarefaction curves in the phase plane, due to the special form of (1.2), which can be written as $Y_t+(uY)_x=0$ [19].

If $\rho_r(u_r-\sigma)=0$, we can conclude that $u_r=u_l=\sigma$ except for $\rho_r=0$ or $\rho_l=0$, which corresponds to a contact discontinuity of the second family. Since λ_2 is linearly degenerate, the sets of states can be connected to a given left state (u_-,ρ_-) by a contact discontinuity on the right if and only if

$$J:\xi=u=u_-. \tag{2.14}$$

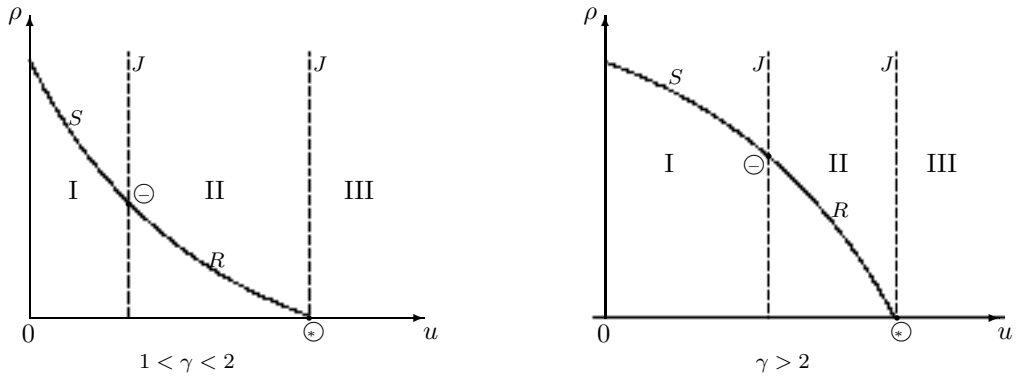

FIG. 2.1.

We note that these waves travel at exactly the same speed as the corresponding cars, which means no information travels faster than the vehicle velocity and the drivers do not react to the traffic situation behind him.

Through the above analysis, we summarize that the sets of states connected on the right consist of the 1-rarefaction wave curve $R(u_-, \rho_-)$, the 1-shock wave curve $S(u_-, \rho_-)$, and the 2-contact discontinuity $J(u_-, \rho_-)$ for a given left state (u_-, ρ_-). These curves divide the quarter phase plane $(u, \rho \geq 0)$ into three regions, $\mathrm{I} = \{(u, \rho) | u < u_-\}$, $\mathrm{II} = \{(u, \rho) | u_- < u < u_*\}$, and $\mathrm{III} = \{(u, \rho) | u > u_*\}$, where $u_* = u_- + \rho_-^{\gamma-1}$ (see Figure 2.1). According to the right state (u_+, ρ_+) in the different region, one can construct the unique global Riemann solution connecting two constant states $(u_\pm, \rho_\pm)$.

Obviously, the Riemann solution contains a 1-shock wave, an intermediate nonvacuum constant state, and a 2-contact discontinuity when $(u_+, \rho_+) \in \mathrm{I}$; it contains a 1-rarefaction wave, an intermediate nonvacuum constant state, and a 2-contact discontinuity when $(u_+, \rho_+) \in \mathrm{II}$; it contains a 1-rarefaction wave, an intermediate vacuum state, and a 2-contact discontinuity when $(u_+, \rho_+) \in \mathrm{III}$.

All of the rarefaction waves R, the shock waves S, and the contact discontinuities J obtained in solving the Riemann problem are called the elementary waves for the AR model (1.2).

3. Interactions of elementary waves. We begin by considering the initial value problem (1.2) with three pieces of constant initial data (1.3). The data (1.3) is a perturbation of the Riemann initial data (2.1). We face the interesting question of determining whether the Riemann solutions of (1.2) and (2.1) are the limits of $(u_\varepsilon, \rho_\varepsilon)(x, t)$ as $\varepsilon \to 0$, where $(u_\varepsilon, \rho_\varepsilon)(x, t)$ are the solutions of (1.2) and (1.3). We will deal with this problem case by case along with constructing the solutions.

We notice that the Riemann solutions of (1.2) and (2.1) may contain the vacuum, so in order to cover all the cases, our discussion should be divided into two parts according to the appearance of vacuum or not. About the interactions of elementary waves not involving the vacuum, we have four cases according to the different combinations of elementary waves from $(-\varepsilon, 0)$ and $(\varepsilon, 0)$ as follows:

1. $R + J$ and $S + J$,
2. $S + J$ and $S + J$,
3. $S + J$ and $R + J$,
4. $R + J$ and $R + J$.

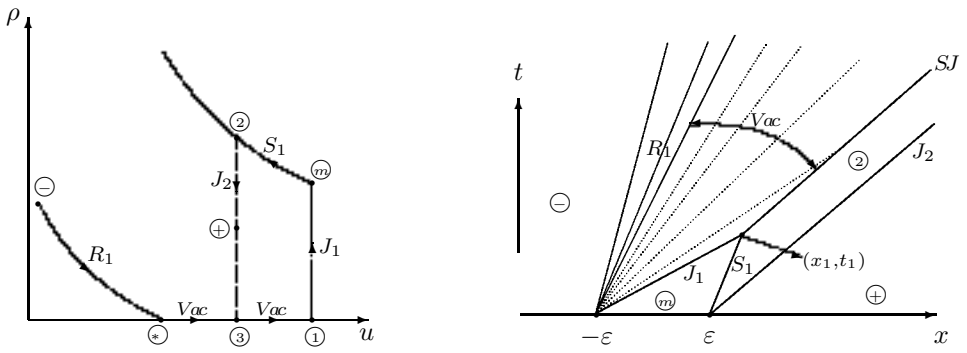

FIG. 3.1.

All the above interactions are classical and well known; hence they will not be pursued here.

In this section, we mainly consider the interactions of elementary waves when at least one of the Riemann solutions at $(-\varepsilon, 0)$ and $(\varepsilon, 0)$ involves the vacuum state. When the Riemann solution contains the vacuum, the AR model (1.2) becomes degenerate in the vacuum region and the two characteristics coincide. In this work, we can study this problem in the (u, ρ) plane, i.e., make a distinction between two vacuum states with different (fake) velocities, like for the method introduced by Liu and Smoller [12] for compressible gas dynamics.

Also, our discussion is divided into the following five cases according to the different combinations of elementary waves from $(-\varepsilon, 0)$ and $(\varepsilon, 0)$:

1. $R + Vac + J$ and $S + J$,
2. $R + Vac + J$ and $R + J$,
3. $R + Vac + J$ and $R + Vac + J$,
4. $R + J$ and $R + Vac + J$,
5. $S + J$ and $R + Vac + J$.

Case 3.1. $R + Vac + J$ and $S + J$.

In this case, when t is small, the solution of the initial value problem (1.2) and (1.3) can be expressed briefly as follows (see Figures 3.1 and 3.2):

$$(u_-, \rho_-) + R_1 + Vac + J_1 + (u_m, \rho_m) + S_1 + (u_2, \rho_2) + J_2 + (u_+, \rho_+),$$

where "+" means "followed by." This case happens if and only if $u_\pm < u_m$ and $u_* = u_- + \rho_-^{\gamma-1} < u_m$.

In the following figures, we just depict the convex situation, i.e., $1 < \gamma < 2$, for the reason that the concave situation is similar.

The propagating speed of J_1 is $\tau_1 = u_m$, and the propagating speed of S_1 is given by

$$\sigma_1 = u_m - \frac{\rho_2(\rho_2^{\gamma-1} - \rho_m^{\gamma-1})}{\rho_2 - \rho_m};$$

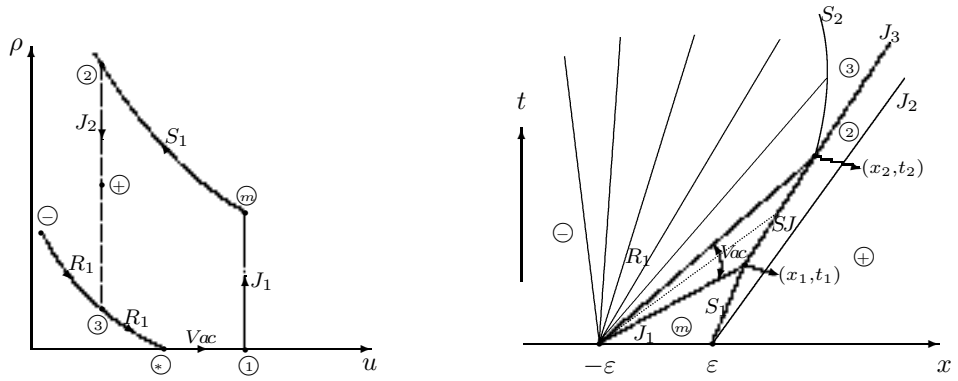

FIG. 3.2.

thus $\tau_1 > \sigma_1$ and the contact discontinuity J_1 will overtake the shock wave S_1 in finite time. The intersection (x_1, t_1) is determined by

$$\begin{cases} x_1 + \varepsilon = u_m t_1, \\ x_1 - \varepsilon = \left(u_m - \dfrac{\rho_2(\rho_2^{\gamma-1} - \rho_m^{\gamma-1})}{\rho_2 - \rho_m} \right) t_1. \end{cases} \tag{3.1}$$

An easy calculation leads to

$$(x_1, t_1) = \left(\frac{2\varepsilon(\rho_2 - \rho_m)u_m}{\rho_2(\rho_2^{\gamma-1} - \rho_m^{\gamma-1})} - \varepsilon, \frac{2\varepsilon(\rho_2 - \rho_m)}{\rho_2(\rho_2^{\gamma-1} - \rho_m^{\gamma-1})} \right). \tag{3.2}$$

It is clear that two elementary waves intersect at a finite time when a new Riemann problem is formed. At the time $t = t_1$, we again have a Riemann problem with data $(u_l, \rho_l) = (u_1, \rho_1)$, $(u_r, \rho_r) = (u_2, \rho_2)$, which is resolved by a new shock S and a new contact discontinuity J. Here we notice that at the left-hand side of S is the vacuum state; thus it is not difficult to see that the propagating speeds of S and J are both equal to u_2; i.e., S and J coincide with each other and form a new wave, which we denote by SJ.

Now, we turn our attention to the interaction of SJ and R_1. It is easy to see that $u_2 = u_+$ and the wave front in R_1 propagates with speed u_*. Our claim is that R_1 and SJ cannot intersect if $u_* \le u_+$ (see Figure 3.1), while for $u_* > u_+$ they must intersect with each other (see Figure 3.2).

If $u_* > u_+$, SJ will cancel the vacuum region and then intersect with R_1 at the point (x_2, t_2), which can be given by

$$\begin{cases} x_2 + \varepsilon = u_* t_2 = (u_- + \rho_-^{\gamma-1})t_2, \\ x_2 - x_1 = u_2(t_2 - t_1). \end{cases} \tag{3.3}$$

Solving the Riemann problem at (x_2, t_2), we can see the appearance of a shock wave S_2 and a contact discontinuity J_3. Namely, when $t > t_2$, SJ decomposes and the state (u_3, ρ_3) lies between S_2 and J_3. At the same time, the shock wave S_2 begins to penetrate R_1 with a varying speed of propagation during the process of penetration;

that is, the shock $S_2 : x = x(t)$ is no longer a straight line at $t > t_2$. The varying speed of S_2 can be determined by

$$\begin{cases} \dfrac{dx}{dt} = u - \dfrac{\rho_3(\rho_3^{\gamma-1} - \rho^{\gamma-1})}{\rho_3 - \rho}, \\ x + \varepsilon = (u - (\gamma-1)\rho^{\gamma-1})t, \\ u - u_- = \rho_-^{\gamma-1} - \rho^{\gamma-1}, \\ x(t_2) = x_2, \quad 0 \le \rho < \rho_3. \end{cases} \tag{3.4}$$

Differentiating the second equation in (3.4) with respect to t, we obtain

$$\frac{dx}{dt} = u - (\gamma-1)\rho^{\gamma-1} + t\Big(\frac{du}{dt} - (\gamma-1)^2\rho^{\gamma-2}\frac{d\rho}{dt}\Big). \tag{3.5}$$

Combining (3.5) with the first equation in (3.4), it is easy to get

$$\frac{(\gamma-1)\rho^\gamma - \gamma\rho_3\rho^{\gamma-1} + \rho_3^\gamma}{\rho - \rho_3} = t\Big(\frac{du}{dt} - (\gamma-1)^2\rho^{\gamma-2}\frac{d\rho}{dt}\Big). \tag{3.6}$$

It follows from the third equation in (3.4) that

$$\frac{du}{dt} = -(\gamma-1)\rho^{\gamma-2}\frac{d\rho}{dt}. \tag{3.7}$$

Substituting (3.7) into (3.6), it yields

$$\frac{d\rho}{dt} = \frac{(\gamma-1)\rho^\gamma - \gamma\rho_3\rho^{\gamma-1} + \rho_3^\gamma}{(\gamma-1)\gamma\rho^{\gamma-2}(\rho_3 - \rho)t}. \tag{3.8}$$

Differentiating the first equation in (3.4), in view of (3.7), (3.8), we have

$$\frac{d^2x}{dt^2} = \frac{((\gamma-1)\rho^\gamma - \gamma\rho_3\rho^{\gamma-1} + \rho_3^\gamma)^2}{(\gamma-1)\gamma\rho^{\gamma-2}(\rho - \rho_3)^3 t}, \tag{3.9}$$

which gives $\frac{d^2x}{dt^2} < 0$ for $\rho < \rho_3$, i.e., S_2 decelerates during the process of penetration.

Integrating (3.8) leads to

$$\ln\frac{t}{t_2} = \int_0^\rho \frac{(\gamma-1)\gamma\rho^{\gamma-2}(\rho_3 - \rho)}{(\gamma-1)\rho^\gamma - \gamma\rho_3\rho^{\gamma-1} + \rho_3^\gamma}d\rho. \tag{3.10}$$

It is clear that $t \to \infty$ as $\rho \to \rho_3$. Therefore, S_2 cannot penetrate over R_1 forever if $\rho_3 \le \rho_-$; otherwise S_2 will cross the whole of R_1 at the finite time

$$t_3 = t_2 \exp\left(\int_0^{\rho_-} \frac{(\gamma-1)\gamma\rho^{\gamma-2}(\rho_3 - \rho)}{(\gamma-1)\rho^\gamma - \gamma\rho_3\rho^{\gamma-1} + \rho_3^\gamma}d\rho\right).$$

Thus we conclude that S_2 is able to cross the whole of R_1 for $\rho_3 > \rho_-$ (i.e., $u_+ < u_-$), whereas it cannot for $\rho_3 \le \rho_-$ (i.e., $u_+ \ge u_-$) and ultimately has $x + \varepsilon = (u_3 - (\gamma-1)\rho_3^{\gamma-1})t$ as its asymptote.

In brief, if $u_+ \ge u_*$, when $t > t_1$, the solution can be expressed as

$$(u_-, \rho_-) + R_1 + Vac + SJ + (u_2, \rho_2) + J_2 + (u_+, \rho_+).$$

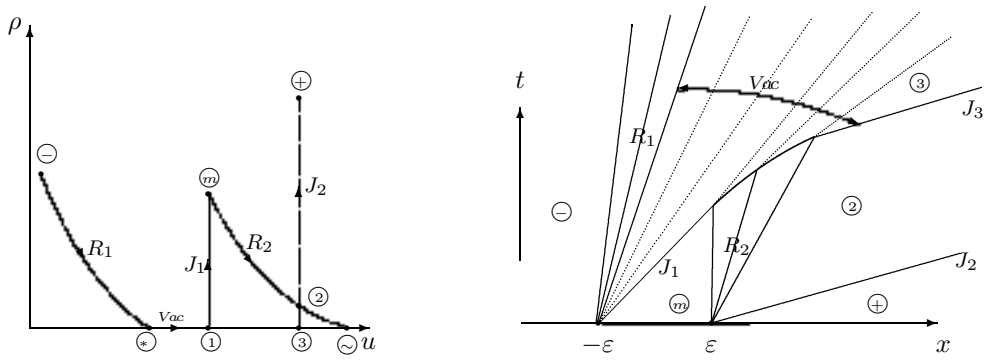

FIG. 3.3.

If $u_+ < u_*$, when $t \to \infty$, the solution can be expressed as

$$(u_-, \rho_-) + R + (u_3, \rho_3) + J_3 + (u_2, \rho_2) + J_2 + (u_+, \rho_+) \quad \text{for } u_+ \geq u_-,$$

$$(u_-, \rho_-) + S + (u_3, \rho_3) + J_3 + (u_2, \rho_2) + J_2 + (u_+, \rho_+) \quad \text{for } u_+ < u_-.$$

Case 3.2. $R + Vac + J$ and $R + J$.

In this case, when t is small, the solution of the initial value problem (1.2) and (1.3) can be expressed briefly as follows (see Figure 3.3):

$$(u_-, \rho_-) + R_1 + Vac + J_1 + (u_m, \rho_m) + R_2 + (u_2, \rho_2) + J_2 + (u_+, \rho_+).$$

This case occurs when $u_* < u_m < u_+ < u_\sim = u_m + \rho_m^{\gamma-1}$ is satisfied.

Obviously, the contact discontinuity J_1 will overtake the rarefaction wave R_2, and they begin to interact with each other at (x_1, t_1), which satisfies

$$\begin{cases} x_1 + \varepsilon = u_m t_1, \\ x_1 - \varepsilon = (u_m - (\gamma-1)\rho_m^{\gamma-1}) t_1. \end{cases} \tag{3.11}$$

This gives

$$(x_1, t_1) = \left(\frac{2\varepsilon u_m - \varepsilon(\gamma-1)\rho_m^{\gamma-1}}{(\gamma-1)\rho_m^{\gamma-1}}, \frac{2\varepsilon}{(\gamma-1)\rho_m^{\gamma-1}} \right). \tag{3.12}$$

Then J_1 goes on to penetrate R_2, and the contact discontinuity $x = x(t)$ during the process of penetration is determined by

$$\begin{cases} \dfrac{dx}{dt} = u, \\ x - \varepsilon = (u - (\gamma-1)\rho^{\gamma-1})t, \\ u - u_m = \rho_m^{\gamma-1} - \rho^{\gamma-1}, \\ x(t_1) = x_1, \quad \rho_2 \leq \rho \leq \rho_m. \end{cases} \tag{3.13}$$

Differentiating (3.13) with respect to t along $x = x(t)$, we obtain

$$\frac{d^2x}{dt^2} = \frac{du}{dt}, \tag{3.14}$$

$$\frac{dx}{dt} = u - (\gamma-1)\rho^{\gamma-1} + \Big(\frac{du}{dt} - (\gamma-1)^2\rho^{\gamma-2}\frac{d\rho}{dt}\Big)t, \tag{3.15}$$

$$\frac{du}{dt} = -(\gamma-1)\rho^{\gamma-2}\frac{d\rho}{dt}. \tag{3.16}$$

Substituting $\frac{dx}{dt} = u$ into the above expressions, it yields

$$\frac{d^2x}{dt^2} = \frac{(\gamma-1)\rho^{\gamma-1}}{\gamma t} > 0,$$

which means that the contact discontinuity accelerates during the process of penetration.

It follows from (3.13) that

$$\frac{dx}{dt} = \frac{x-\varepsilon}{t} + (\gamma-1)\rho^{\gamma-1} = \frac{x-\varepsilon}{t} + (\gamma-1)\Big(\rho_m^{\gamma-1} + u_m - \frac{dx}{dt}\Big).$$

So (3.13) can be simplified as

$$\begin{cases} \dfrac{dx}{dt} = \dfrac{x-\varepsilon}{\gamma t} + \dfrac{\gamma-1}{\gamma}(u_m + \rho_m^{\gamma-1}), \\ x(t_1) = x_1. \end{cases} \tag{3.17}$$

By applying the method of variation of constant, we obtain

$$x = \varepsilon + (u_m + \rho_m^{\gamma-1})t - \gamma\Big(\frac{2\varepsilon\rho_m}{\gamma-1}\Big)^{1-\frac{1}{\gamma}} t^{\frac{1}{\gamma}}, \tag{3.18}$$

which, together with

$$x - \varepsilon = (u_2 - (\gamma-1)\rho_2^{\gamma-1})t, \tag{3.19}$$

determines the ending point (x_2, t_2) of the penetration. A direct calculation leads to

$$(x_2, t_2) = \Big(\varepsilon + \frac{2\varepsilon\rho_m u_2}{(\gamma-1)\rho_2^{\gamma}} - \frac{2\varepsilon\rho_m}{\rho_2}, \frac{2\varepsilon\rho_m}{(\gamma-1)\rho_2^{\gamma}}\Big). \tag{3.20}$$

It turns out that the contact discontinuity J_1 crosses the rarefaction wave R_2 completely in finite time and R_2 becomes the vacuum state after penetration.

For large time, the solution can be expressed as

$$(u_-, \rho_-) + R_1 + Vac + J_3 + (u_2, \rho_2) + J_2 + (u_+, \rho_+).$$

Case 3.3. $R + Vac + J$ and $R + Vac + J$.

In this case, when t is small, the solutions of the initial value problems (1.2) and (1.3) can be expressed briefly as follows (see Figure 3.4):

$$(u_-, \rho_-) + R_1 + Vac + J_1 + (u_m, \rho_m) + R_2 + Vac + J_2 + (u_+, \rho_+).$$

The occurrence of this case depends on the condition $u_* < u_m < u_\sim < u_+$.

Indeed, this case is similar to Case 3.2 except that the vacuum states appear in front of R_2 at the beginning. In the same way as before, we can see that the

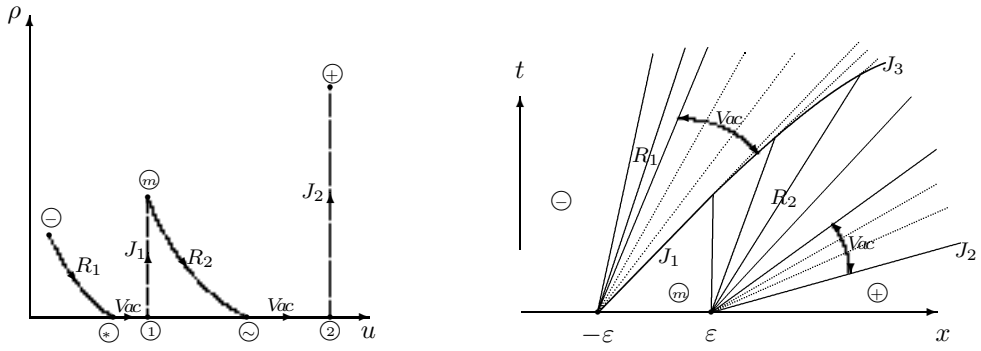

FIG. 3.4.

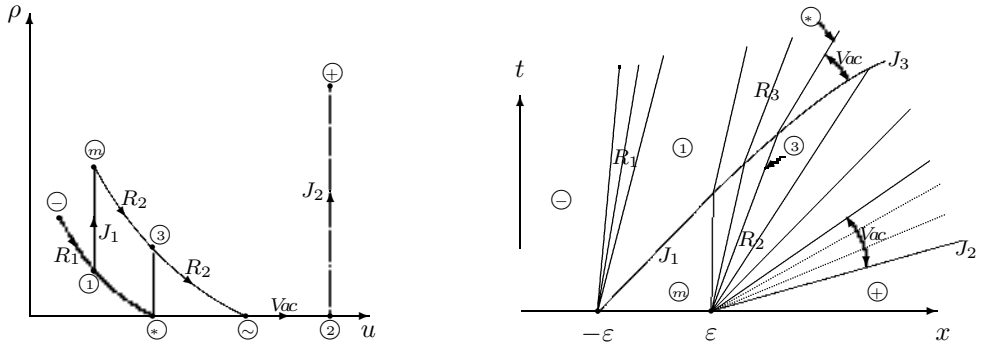

FIG. 3.5.

propagating speed of J_3 tends to $u_\sim$ as $t \to \infty$; i.e., J_3 has the wave front in R_2 as its asymptote.

As $t \to \infty$, the time-asymptotic solution can be described as

$$(u_-, \rho_-) + R_1 + Vac + J_2 + (u_+, \rho_+).$$

Case 3.4. $R + J$ and $R + Vac + J$.

In this case, when t is small, the solutions of the initial value problems (1.2) and (1.3) can be expressed briefly as follows (see Figure 3.5):

$$(u_-, \rho_-) + R_1 + (u_1, \rho_1) + J_1 + (u_m, \rho_m) + R_2 + Vac + J_2 + (u_+, \rho_+).$$

This case happens when $u_- < u_m < u_*$ and $u_+ > u_\sim$ are satisfied.

This case can be discussed similarly to Case 3.3. Moreover, it can be shown that the vacuum states form ahead of R_3 at the time when one of the states in R_2 becomes (u_3, ρ_3). Then, J_3 continues to penetrate R_2 and finally disappears in the vacuum as $t \to \infty$.

For large time, the solution can be expressed as

$$(u_-, \rho_-) + R_1 + (u_1, \rho_1) + R_3 + Vac + J_2 + (u_+, \rho_+).$$

Case 3.5. $S + J$ and $R + Vac + J$.

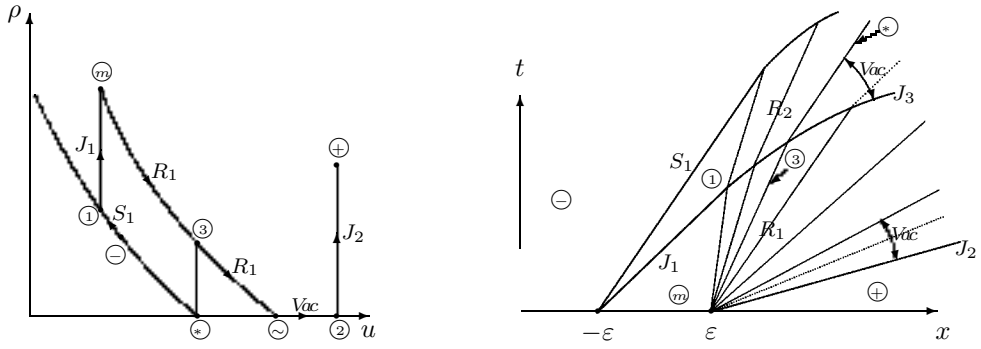

FIG. 3.6.

In this case, when t is small, the solutions of the initial value problems (1.2) and (1.3) can be expressed briefly as follows (see Figure 3.6):

$$(u_-, \rho_-) + S_1 + (u_1, \rho_1) + J_1 + (u_m, \rho_m) + R_1 + Vac + J_2 + (u_+, \rho_+).$$

The appearance of this case depends on the conditions $u_m < u_-$ and $u_\sim < u_+$.

Like for Case 3.4, the interaction of J_1 and R_1 results in a new contact discontinuity J_3 and a new rarefaction wave R_2. Similarly, the vacuum states present ahead of R_2 at the time when one of the states in R_1 turns to be (u_3, ρ_3). The propagating speed of J_3 tends to $u_\sim$ as $t \to \infty$; i.e., J_3 has the wave front in R_1 as its asymptote.

Now we mainly consider the interaction of the shock wave S_1 and the rarefaction wave R_2. The propagating speed of S_1 is

$$\sigma_1 = u_- - \frac{\rho_1(\rho_1^{\gamma-1} - \rho_-^{\gamma-1})}{\rho_1 - \rho_-},$$

and the propagating speed of the wave back in R_2 is $\omega_2 = u_1 - (\gamma-1)\rho_1^{\gamma-1}$. Noting $u_1 - u_- = \rho_-^{\gamma-1} - \rho_1^{\gamma-1}$, it is easy to get

$$\sigma_1 - \omega_2 = \frac{(\gamma-1)\rho_1^\gamma - \gamma\rho_-\rho_1^{\gamma-1} + \rho_-^\gamma}{\rho_1 - \rho_-}. \tag{3.21}$$

Define $x = \frac{\rho_1}{\rho_-} > 1$ and introduce $f(x) = (\gamma-1)x^\gamma - \gamma x^{\gamma-1} + 1$; then one can easily see that

$$\sigma_1 - \omega_2 = \frac{\rho_-^\gamma}{\rho_1 - \rho_-} f(x).$$

Obviously, we have $f'(x) = (\gamma-1)\gamma x^{\gamma-2}(x-1) > 0$ for $x > 1$, which gives $f(x) > f(1) = 0$ and then $\sigma_1 > \omega_2$. Thus S_1 will overtake R_2 in finite time and the intersection (x_2, t_2) can be calculated by

$$\begin{cases} x_2 + \varepsilon = \Big(u_- - \dfrac{\rho_1(\rho_1^{\gamma-1} - \rho_-^{\gamma-1})}{\rho_1 - \rho_-}\Big)t_2, \\ x_2 - x_1 = (u_1 - (\gamma-1)\rho_1^{\gamma-1})(t_2 - t_1), \end{cases} \tag{3.22}$$

in which (x_1, t_1) has the same representation as (3.12).

Hence, (x_2, t_2) can be expressed as

$$(x_2,t_2)=\Big(\frac{2\varepsilon[\rho_1^{\gamma-1}(\rho_1-\rho_-)-\rho_1^{\gamma}(\rho_1^{\gamma-1}-\rho_-^{\gamma-1})]}{\rho_m^{\gamma-1}[(\gamma-1)\rho_1^{\gamma}-\gamma\rho_-\rho_1^{\gamma-1}+\rho_-^{\gamma}]}-\varepsilon,\frac{2\varepsilon\rho_1^{\gamma-1}(\rho_1-\rho_-)}{\rho_m^{\gamma-1}[(\gamma-1)\rho_1^{\gamma}-\gamma\rho_-\rho_1^{\gamma-1}+\rho_-^{\gamma}]}\Big).$$

When $t>t_2$, S_1 begins to penetrate R_2, and the shock wave $x=x(t)$ during the process of penetration satisfies

$$\begin{cases}\dfrac{dx}{dt}=u_--\dfrac{\rho(\rho^{\gamma-1}-\rho_-^{\gamma-1})}{\rho-\rho_-},\\ x-\hat{x}=(u-(\gamma-1)\rho^{\gamma-1})(t-\hat{t}),\\ u-u_1=\rho_1^{\gamma-1}-\rho^{\gamma-1},\\ x(t_2)=x_2,\quad 0\le\rho\le\rho_1,\end{cases}\tag{3.23}$$

in which $(\hat{x},\hat{t})$ are the translation points from R_1 to R_2 and can be calculated by (3.13), but here $\rho_3\le\rho\le\rho_m$.

Similarly, by differentiating (3.23) with respect to t along $x=x(t)$ and noting that $u-u_-=-\rho^{\gamma-1}+\rho_-^{\gamma-1}$, we finally obtain, for $\rho>\rho_-$,

$$\frac{d\rho}{dt}=-\frac{(\gamma-1)\rho^{\gamma}-\gamma\rho_-\rho^{\gamma-1}+\rho_-^{\gamma}}{(\gamma-1)\gamma\rho^{\gamma-2}(\rho-\rho_-)(t-\hat{t})}<0,\tag{3.24}$$

$$\begin{aligned}\frac{d^2x}{dt^2}&=-\frac{(\gamma-1)\rho^{\gamma}-\gamma\rho_-\rho^{\gamma-1}+\rho_-^{\gamma}}{(\rho-\rho_-)^2}\cdot\frac{d\rho}{dt}\\ &=\frac{((\gamma-1)\rho^{\gamma}-\gamma\rho_-\rho^{\gamma-1}+\rho_-^{\gamma})^2}{(\gamma-1)\gamma\rho^{\gamma-2}(\rho-\rho_-)^3(t-\hat{t})}>0,\end{aligned}\tag{3.25}$$

which means that the shock wave accelerates during the process of penetration.

Integrating (3.24) yields

$$\ln\frac{t-\hat{t}}{t_2-\hat{t}}=-\int_{\rho_1}^{\rho}\frac{(\gamma-1)\gamma\rho^{\gamma-2}(\rho-\rho_-)}{(\gamma-1)\rho^{\gamma}-\gamma\rho_-\rho^{\gamma-1}+\rho_-^{\gamma}}d\rho,\tag{3.26}$$

and we see that $t\to\infty$ as $\rho\to\rho_-$. Therefore, S_1 cannot penetrate over R_2 forever and the propagating speed of the shock wave will tend to $u_--(\gamma-1)\rho_-^{\gamma-1}$ as $t\to\infty$.

In brief, when $t\to\infty$, the solution can be expressed as

$$(u_-,\rho_-)+R+Vac+J_2+(u_+,\rho_+).$$

Remark 1. The curve passing through (u_-,ρ_-) is below the one passing through (u_m,ρ_m) if $u_-+\rho_-^{\gamma-1}<u_m+\rho_m^{\gamma-1}$ (i.e., $u_*<u_\sim$) in the (u,ρ) plane; otherwise the situation is opposite. Here we select the situation $u_*<u_\sim$ to discuss, and the other can be dealt with similarly.

4. Stability analysis and comparison. In this section, let us first consider whether the limits of the perturbed solutions of (1.2) and (1.3) are the corresponding Riemann solutions of (1.2) and (2.1). It is obviously true when the vacuum is not involved. On the other hand, if the vacuum is involved, let us take Case 3.1 as an example to study the limit situations of the above perturbed solutions for details.

In Case 3.1, it can be easily derived from (3.2) that $(x_1, t_1) \to (0, 0)$ as $\varepsilon \to 0$; thus the three points $(-\varepsilon, 0)$, $(\varepsilon, 0)$, and (x_1, t_1) coincide with each other in the limit situation. If $u_+ \geq u_* > u_-$ (see Figure 3.1), as $\varepsilon \to 0$, the intermediate state (u_2, ρ_2) disappears while SJ and J_2 unify into one contact discontinuity J since SJ and J_2 propagate with the same speed u_+. So the structure of the solution tends to $(u_-, \rho_-)+R+Vac+J+(u_+, \rho_+)$ as $\varepsilon \to 0$. Otherwise, if $u_+ < u_*$ (see Figure 3.2), we can also see that $(x_2, t_2) \to (0, 0)$ as $\varepsilon \to 0$ from (3.3) and the vacuum state disappears in the limit situation. Furthermore, S_2 cannot penetrate over R_1 for $u_- \leq u_+$, and the limit of the perturbed solution is $(u_-, \rho_-) + R + (u_3, \rho_3) + J + (u_+, \rho_+)$. Otherwise, S_2 is able to penetrate the whole of R_1 for $u_+ < u_-$, and the limit situation is $(u_-, \rho_-) + S + (u_3, \rho_3) + J + (u_+, \rho_+)$.

Therefore, in Case 3.1 the Riemann solutions are claimed to be stable for such perturbations with the Riemann data (2.1). The other cases can be analyzed similarly. Hence, we can see that the limits of the solutions of the perturbed Riemann problems (1.2) and (1.3) are exactly the solutions of the corresponding Riemann problems (1.2) and (2.1), which shows the stability of the Riemann solutions with respect to the small perturbations of the initial data in this particular situation.

In [2], Aw and Rascle considered the Riemann problem when the left (or right) state is the vacuum state and they fixed the right (or left) state and slightly perturbed the left (or right) state so that $0 < \rho_- \ll 1$ (or $0 < \rho_+ \ll 1$). They discovered that a big oscillation appeared and the solution dramatically changed under their small perturbations in some cases. Thus, the Riemann solution displays the instability when one of the Riemann data is near the vacuum under their perturbations. In [11], Lebacque, Mammer, and Haj-Salem extended properly the fundamental diagram (equilibrium speed-density relationship) in a suitable fashion to solve the Riemann problem for all initial conditions and to avoid irregular behavior at the low densities pointed out by Aw and Rascle.

If we adopt the perturbation such as (1.3), the stability of the Riemann solution can be obtained under the assumption $\rho_\pm > 0$ in section 3. Indeed, this stability can also be arrived at when one of the Riemann data is the vacuum state. Now, in order to compare with the results in [2], let us reconsider two interesting and typical examples: the perturbation (iv) of case 5 and the perturbation (vii) of case 4 (both in [2]).

Case 4.1. Let us first consider the perturbation (iv) of case 5 in [2]. In this case, the Riemann problem has no traffic on the left: $\rho_- = 0$, and the initial data on the right satisfies $u_+ < u_- < u_\star = u_+ + \rho_+^{\gamma-1}$. According to [2], for $\rho_- = 0$, the Riemann problem can be connected by a 2-contact discontinuity directly and the wave of the first family disappears. The shock with the large amplitude presents, and the Riemann solution is obviously unstable under the perturbation proposed by Aw and Rascle. But we can see that the Riemann solution is still stable if we take the perturbation (u_m, ρ_m) in the interval $(-\varepsilon, \varepsilon)$. According to the value of u_m, we divide our discussion into the following two subcases.

Subcase 4.1.1. If $u_+ < u_m$, then J_1 emerges from $(-\varepsilon, 0)$ and S_1 and J_2 start from $(\varepsilon, 0)$ (see Figure 4.1). Like in Case 3.1, J_1 must overtake S_1 in finite time and they unify into a contact discontinuity J_3 with the velocity u_+.

Subcase 4.1.2. If $u_+ > u_m$, then J_1 emerges from $(-\varepsilon, 0)$ and R_1 and J_2 emanate from $(\varepsilon, 0)$ (see Figure 4.2). Similarly to Case 3.2, J_1 will penetrate R_1 completely in finite time and then be denoted by J_3 with the velocity u_+, and R_1 will become the vacuum state at the same time.

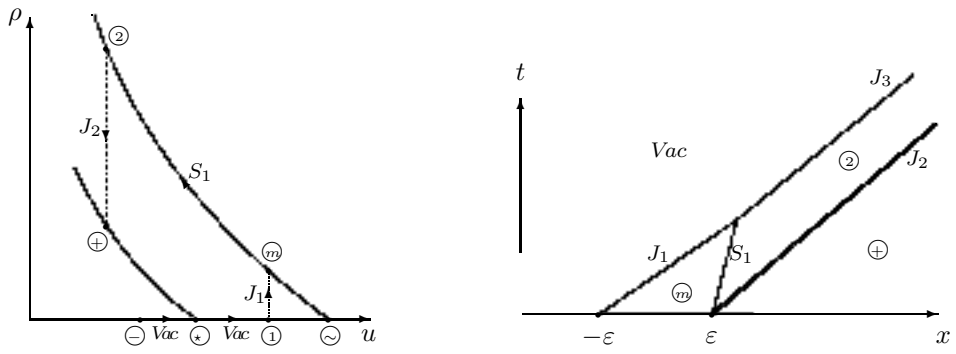

FIG. 4.1.

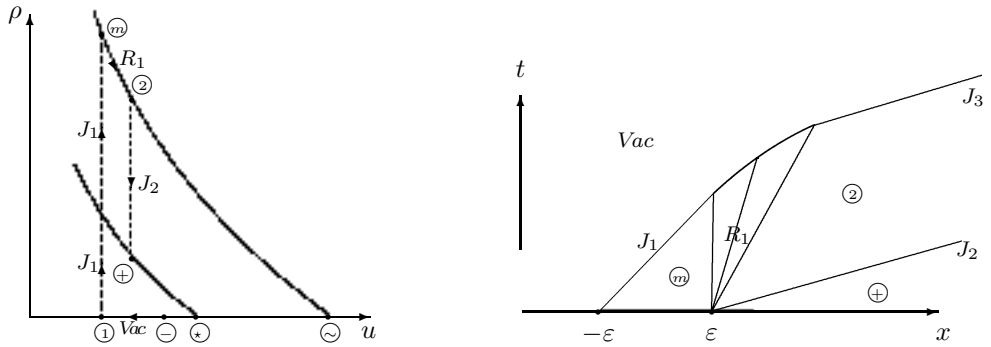

FIG. 4.2.

Remark 2. If $\rho_- = 0$ and $u_+ < u_-$, we can also believe that the Riemann solution consists of a 1-shock S connecting $(u_-, 0)$ and $(u_+, \sqrt[\gamma-1]{u_- - u_+})$, followed by a 2-contact discontinuity J connecting $(u_+, \sqrt[\gamma-1]{u_- - u_+})$ and (u_+, ρ_+). But S and J propagate at the same speed u_+; thus they coalesce into a new wave SJ and the intermediate state $(u_+, \sqrt[\gamma-1]{u_- - u_+})$ disappears in the (x, t) plane. The new wave SJ has the same properties as J and can also be regarded as J. Otherwise, if $\rho_- = 0$ and $u_+ > u_-$, it can also be believed that the Riemann solution consists of a fake vacuum wave connecting the two vacuum states $(u_-, 0)$ and $(u_+, 0)$ and then followed by a contact discontinuity J connecting $(u_+, 0)$ and (u_+, ρ_+).

Case 4.2. Let us now come back to the perturbation (vii) of case 4 in [2]. In this case, the Riemann data satisfies $\rho_+ = 0$ and $u_+ < u_-$. Based on [2], for $\rho_+ = 0$, the Riemann solution consists only of a rarefaction wave and there is no need to add a contact discontinuity. If we employ the perturbation in [2], the perturbed solution is still more dramatically different from the original one in that a (possible large) shock wave and a large contact discontinuity appear. However, we can see that the Riemann solution is still stable if we adopt the perturbation (1.3). Our discussion is also divided into the following two subcases according to the value of u_m.

Subcase 4.2.1. If $u_- < u_m$, then R_1 and J_1 generate from $(-\varepsilon, 0)$ and R_2 emanates from $(\varepsilon, 0)$. If $u_m \le u_*$, as in Case 3.4, the vacuum state will form ahead of R_3 when one of the states in R_2 becomes (u_2, ρ_2). J_1 penetrates R_2 and has $x - \varepsilon = u_\sim t$ as its

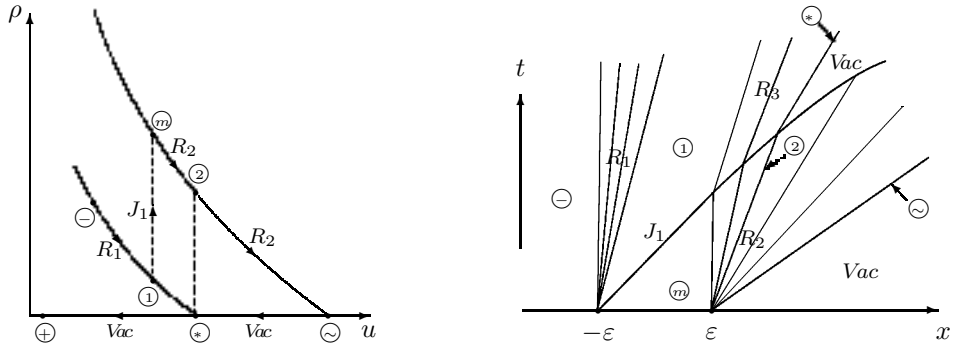

FIG. 4.3. $(u_+ <) u_- < u_m \le u_*$.

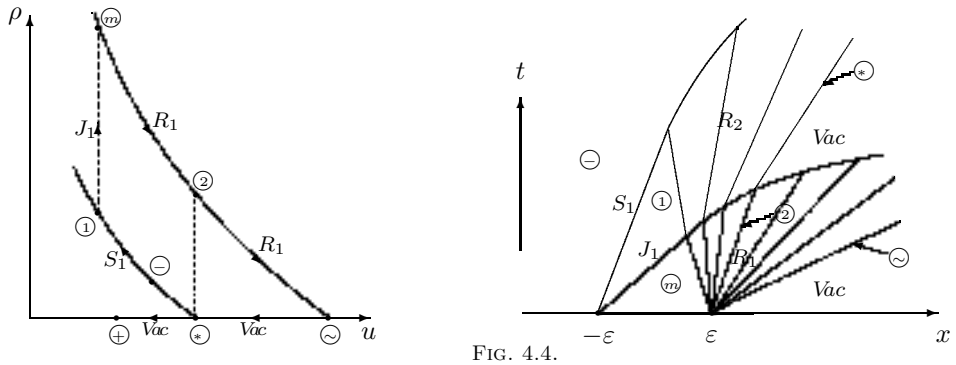

FIG. 4.4.

asymptote, which finally disappears at infinity for both sides are the vacuum states (see Figure 4.3). For the remaining case $u_m > u_*$, the conclusion is analogous and the difference lies in that R_3 disappears and the intermediate state between R_1 and J_1 becomes the vacuum state.

Subcase 4.2.2. If $u_- > u_m$, then S_1 and J_1 generate from $(-\varepsilon, 0)$ and R_1 emits from $(\varepsilon, 0)$. With the same reasoning as before, J_1 penetrates R_1 and has the wave front in R_1 as its asymptote; eventually it disappears in the vacuum as $t \to \infty$. For S_1, it cannot penetrate R_2 completely and its speed tends to $u_- - (\gamma - 1)\rho_-^{\gamma-1}$ in the end (see Figure 4.4).

Remark 3. If $\rho_+ = 0$ and $u_+ < u_-$ (or $u_- < u_+ < u_*$), we can also believe the Riemann solution consists of a 1-shock wave S (or a 1-rarefaction wave R) connecting (u_-, ρ_-) and $(u_+, \sqrt[\gamma-1]{u_- + \rho_-^{\gamma-1} - u_+})$ and then followed by a 2-contact discontinuity J connecting $(u_+, \sqrt[\gamma-1]{u_- + \rho_-^{\gamma-1} - u_+})$ and $(u_+, 0)$. Otherwise, if $\rho_+ = 0$ and $u_+ > u_*$, we can believe that the Riemann solution consists of a 1-rarefaction wave R connecting (u_-, ρ_-) and $(u_*, 0)$ and then followed by a fake vacuum wave connecting the two vacuum states $(u_*, 0)$ and $(u_+, 0)$.

By letting $\varepsilon \to 0$, it is easy to see that the Riemann solutions are stable under the perturbations (1.3) in the above two cases. The other cases in [2] can be treated in the same way, and the results are also identical with our assertions. It should be pointed out that the perturbations adopted in this paper are local perturbations, which are

obviously different from the perturbations proposed by Aw and Rascle. This may be used to explain the following traffic situation: the perturbation of traffic status in a small range will come back soon.

5. Conclusion. So far, the discussion for all kinds of interactions has been completed. We have globally constructed the solutions for the perturbed initial value problem (1.2) and (1.3). From the above analysis, we can find that the asymptotic behavior of the perturbed solutions is governed completely by the states $(u_\pm, \rho_\pm)$. That is, the elementary waves in the time-asymptotic solutions consist of R and J for $u_+ > u_-$, or S and J for $u_+ < u_-$. Particularly, for $u_- < u_* < u_+$, the vacuum states are involved as the intermediate states between R and J in the time-asymptotic solutions. Thus we can draw the conclusion that the Riemann solutions of (1.2) and (2.1) are stable with respect to the small perturbations of the initial data in this particular situation.

REFERENCES

[1] A. Aw, A. Klar, A. Materne, and M. Rascle, *Derivation of continuum traffic flow models from microscopic follow-the-leader model*, SIAM J. Appl. Math., 63 (2002), pp. 259–278.

[2] A. Aw and M. Rascle, *Resurrection of "second order" models of traffic flow*, SIAM J. Appl. Math., 60 (2000), pp. 916–938.

[3] F. Berthelin, P. Degond, M. Delitata, and M. Rascle, *A model for the formation and evolution of traffic jams*, Arch. Ration. Mech. Anal., 187 (2008), pp. 185–220.

[4] T. Chang and L. Hsiao, *The Riemann Problem and Interaction of Waves in Gas Dynamics*, Pitman Monographs and Surveys in Pure and Applied Mathematics 41, Longman Scientific and Technical, Harlow, UK, 1989.

[5] C. M. Dafermos, *Hyperbolic Conservation Laws in Continuum Physics*, Grundlehren Math. Wiss., Springer-Verlag, Berlin, 2000.

[6] C. Daganzo, *Requiem for second order fluid approximations of traffic flow*, Transportation Res. B, 29 (1995), pp. 277–286.

[7] M. Garavello and B. Piccoli, *Traffic flow on a road network using the Aw–Rascle model*, Comm. Partial Differential Equations, 31 (2006), pp. 243–275.

[8] J. M. Greenberg, *Extensions and amplifications of a traffic model of Aw and Rascle*, SIAM J. Appl. Math., 62 (2001), pp. 729–745.

[9] J. M. Greenberg, A. Klar, and M. Rascle, *Congestion on multilane highways*, SIAM J. Appl. Math., 63 (2003), pp. 818–833.

[10] M. Herty and M. Rascle, *Coupling conditions for a class of second-order models for traffic flow*, SIAM J. Math. Anal, 38 (2006), pp. 595–616.

[11] J. P. Lebacque, S. Mammer, and H. Haj-Salem, *The Aw–Rascle and Zhang's model: Vacuum problems, existence and regularity of the solutions of the Riemann problem*, Transportation Res. B, 41 (2007), pp. 710–721.

[12] T. P. Liu and J. Smoller, *On the vacuum state for isentropic gas dynamic equations*, Adv. in Appl. Math., 1 (1980), pp. 345–359.

[13] S. Moutari and M. Rascle, *A hybrid Lagrangian model based on the Aw–Rascle traffic flow model*, SIAM J. Appl. Math., 68 (2007), pp. 413–436.

[14] D. Serre, *Systems of Conservation Laws,* 1 *and* 2, Cambridge University Press, Cambridge, UK, 1999 and 2000.

[15] C. Shen and M. Sun, *Formation of Delta-Shocks and Vacuum States in the Vanishing Pressure Limit of Solutions to the Aw–Rascle Model*, submitted.

[16] W. Sheng, M. Sun, and T. Zhang, *The generalized Riemann problem for a scalar nonconvex Chapman–Jouguet combustion model*, SIAM J. Appl. Math., 68 (2007), pp. 544–561.

[17] J. Smoller, *Shock Waves and Reaction-Diffusion Equations*, 2nd ed., Springer-Verlag, New York, 1994.

[18] M. Sun and W. Sheng, *The ignition problem for a scalar nonconvex combustion model*, J. Differential Equations, 231 (2006), pp. 673–692.

[19] B. Temple, *Systems of conservation laws with coinciding shock and rarefaction curves*, Contemp. Math., 17 (1983), pp. 143–151.

[20] M. Zhang, *A non-equilibrium traffic model devoid of gas-like behavior*, Transportation Res. B, 36 (2002), pp. 275–290.